

# Sensitivity of Hydrogen Bond Lifetime Dynamics to the Presence of Ethanol at the Interface of a Phospholipid Bilayer<sup>†</sup>

Jnanojjal Chanda, Sudip Chakraborty, and Sanjoy Bandyopadhyay\*

Molecular Modeling Laboratory, Department of Chemistry, Indian Institute of Technology, Kharagpur 721302, India

Received: August 2, 2005; In Final Form: November 6, 2005

Atomistic molecular dynamics simulations of a fully hydrated liquid crystalline lamellar phase of a dimyristoylphosphatidylcholine lipid bilayer containing ethanol at 1:1 composition as well as of the pure lamellar phase of the bilayer have been performed. Detailed analyses have been carried out to investigate the effects of ethanol, if any, on the lifetime dynamics of lipid–water and water–water hydrogen bonds in the hydration layer of the lipid headgroups. The nonexponential hydrogen bond lifetime correlation functions have been analyzed by using the formalism of Luzar and Chandler, which allowed the identification of the bound states at the bilayer interface and the quantification of the dynamic equilibrium between the bound and the free water molecules, in terms of time-dependent relaxation rates. The calculations show that the overall relaxation of phosphate–water hydrogen bonds is faster in the presence of ethanol. Studies of the residence time and the number fluctuation of the hydration layer water molecules reveal that the presence of ethanol molecules decreases the rigidity of the lipid hydration layer.

## 1. Introduction

The presence of an extended network of hydrogen bonds in liquid water is responsible for many exotic structural and dynamical properties of water.<sup>1–3</sup> The formation and breaking of hydrogen bonds play a crucial role in determining the dynamical properties of water.<sup>4</sup> Although a considerable effort has been made over past several decades to study hydrogen bond dynamics in liquid water,<sup>4–10</sup> a proper microscopic level understanding of the problem is still far from being complete. The dynamics of hydrogen bonds can be probed and interpreted only qualitatively by different experimental techniques, such as Raman scattering, depolarized light scattering, inelastic neutron scattering, ultrafast IR spectroscopy, etc.<sup>7,11–17</sup> Molecular dynamics (MD) simulations, however, can provide quantitative information on hydrogen bond dynamics with atomistic resolution. The factors influencing the dynamics can be ascertained from MD trajectories by calculating different hydrogen bond time correlation functions, as proposed first by Stillinger<sup>4</sup> and developed further by Luzar and Chandler.<sup>5,6</sup> In recent years, there have been a number of simulation studies that have primarily focused on the relaxation behavior of hydrogen bonds in pure water as well as in aqueous solutions of electrolytes and micelles.<sup>5,6,8–10,18–25</sup> These simulation studies in general have shown that the relaxation behavior of hydrogen bonds in liquid water is nonexponential in nature. Recently, Luzar and Chandler<sup>5,6</sup> have proposed a simple model to describe the kinetics of hydrogen bonds in water. The model treats the hydrogen bond dynamics as an activated process, where the rate of relaxation is characterized by a reactive flux correlation function formalism. These studies revealed that the nonexponential relaxation behavior at long times arises due to the coupling of hydrogen bond dynamics and the diffusional motion of water.<sup>5</sup>

The regular hydrogen bond network in pure water gets disrupted in an aqueous solution containing organized molecular assemblies, such as phospholipid membranes. The nature of interactions between membrane components and water is an important issue, as it is believed that water plays an important role in determining the structure, stability, and function of the membrane. Over the past several years, MD simulations have been successfully employed to study the properties of pure model membranes.<sup>26–32</sup> Studies on the influence of various impurities on regular membrane properties have also been reported in recent times.<sup>33–36</sup> Klein and co-workers<sup>33,34</sup> have studied in great detail the distribution of small anesthetics in phospholipid bilayers and its influence on the bilayer properties at different concentrations. Only recently, we carried out detailed MD simulations to study the distribution of ethanol at different concentrations in a phospholipid bilayer containing saturated dimyristoylphosphatidylcholine (DMPC) lipids and its influence on regular bilayer properties.<sup>35,36</sup> It was observed that irrespective of its concentration ethanol molecules interact strongly with the phosphocholine headgroups of the lipids and preferentially occupy regions near the bilayer–water interface.

Such preferential occupation of ethanol molecules at the bilayer interface is likely to influence the regular hydrogen bond network at the interface. In this work, we have studied in detail the effects of ethanol on the dynamics of lipid–water and water–water hydrogen bonds in the hydration layer of the DMPC bilayer in its liquid crystalline lamellar phase ( $L_\alpha$ ). In the recent past, there have been few attempts to study the hydrogen bond properties at the interface of pure phospholipid bilayers.<sup>28–30</sup> However, to the best of our knowledge, this is the first attempt to study the effects of the presence of an impurity on the regular hydrogen bond dynamics of a phospholipid bilayer. We have organized the article as follows. In the next section, we discuss the system setup and the simulation methods employed. The results obtained from our investigations are presented and discussed in the following section. In the last

<sup>†</sup> Part of the special issue “Michael L. Klein Festschrift”.

\* Author to whom correspondence should be addressed. Phone: 91-3222-283344. Fax: 91-3222-255303. E-mail: sanjoy@chem.iitkgp.ernet.in.

section, we summarize the important findings and the conclusions reached from our study.

## 2. System Setup and Simulation Details

Two different simulations were carried out. In the first simulation, a fully hydrated lamellar phase of pure DMPC lipid was studied. This lipid bilayer (we denote it as the “pure” simulation system in this work) was used as the model membrane. The choice of the lipid was motivated by the fact that the system is in the biologically relevant liquid crystalline phase at room temperature.<sup>37</sup> The system contained 64 lipid molecules (32 per leaflet) and an aqueous layer separating the lipid headgroups containing 1645 water molecules. This composition corresponds to a fully hydrated DMPC lipid bilayer at 30 °C with water per lipid molecule,  $n_w = 25.7$ .<sup>37</sup> The system was then equilibrated at constant temperature ( $T = 30$  °C) and pressure ( $P = 1$  atm) (NPT) for 1 ns. This equilibration period was followed by an NPT production run of 4 ns in duration. A well-equilibrated configuration was taken from this simulation to set up the configuration of the DMPC/ethanol bilayer system. The 64 ethanol molecules were uniformly distributed within the bilayer (32 per leaflet or 1:1 composition). We denote this simulation as the “mixed” bilayer system in this work. To avoid unfavorable repulsive contacts with the lipids, the ethanol molecules were initially treated as small point masses with zero atomic charges and van der Waals parameters. Through the use of short consecutive MD runs, the molecules were “grown” in size by extending their intramolecular bonds and their interactions with lipid molecules. This is a convenient way to introduce impurities in a bilayer without inducing large perturbations of the bilayer structure at the beginning of the simulation.<sup>33,34</sup> A short MD run of 50 ps was first carried out by keeping the water molecules fixed at their starting locations. Next, the water molecules were allowed to move, and the system was equilibrated at constant volume and temperature (30 °C) for about 100 ps. The equilibration was continued further for another 1 ns duration at constant temperature (30 °C) and pressure (1 atm). This was followed by approximately 4 ns of an NPT production run, during which the trajectories were stored for subsequent analyses. All of the NPT simulations were performed using flexible simulation cells with orthorhombic angular constraints.<sup>38</sup>

The simulations utilized the Nosé–Hoover chain thermostat extended system method<sup>38</sup> as implemented in the PINY-MD computational package.<sup>39</sup> A recently developed reversible multiple time step algorithm, RESPA,<sup>38</sup> allowed us to employ a MD time step of 4 fs. This was achieved using a three-stage force decomposition into intramolecular forces (torsion/bend–bond), short-range intermolecular forces (a 7.0 Å RESPA cutoff distance), and long-range intermolecular forces. Electrostatic interactions were calculated by using the particle-mesh Ewald (PME) method.<sup>40</sup> The PME and RESPA were combined following the method suggested by Procacci et al.<sup>41</sup> The minimum image convention<sup>42</sup> was employed to calculate the Lennard-Jones interactions and the real-space part of the Ewald sum, using spherical truncations of 7 and 10 Å, respectively, for the short- and the long-range parts of the force decomposition. “SHAKE/ROLL” and “RATTLE/ROLL” methods<sup>38</sup> were implemented to constrain all bonds involving hydrogen atoms to their equilibrium values. We have employed CHARMM27 all-atom force fields and potential parameters for the lipid and ethanol molecules,<sup>43</sup> while the TIP3P model<sup>44</sup> was employed for water, which is consistent with the chosen lipid and ethanol force fields.

## 3. Results and Discussion

The dynamics of water molecules and their structural organization at the interface of a phospholipid bilayer are correlated with the network of hydrogen bonds formed between them and the phosphocholine headgroups of the lipid molecules.<sup>28,29</sup> The probability of formation of hydrogen bonds with water is much higher for the lipid phosphate groups, as they are more accessible to the water molecules.<sup>29</sup> The formation and breaking of these phosphate–water hydrogen bonds are likely to play an important role in determining the structure, stability, and function of a membrane. Generally, either a geometric<sup>28,29</sup> or an energetic<sup>45,46</sup> criterion is used to define a hydrogen bond. In this work, we have employed a purely geometric criterion adopted from earlier studies to define a hydrogen bond.<sup>28,29</sup> According to the definition, a hydrogen bond exists between two oxygen atoms if the distance between them is less than 3.25 Å and the angle between this vector and one O–H bond is less than 35°.

The dynamics of hydrogen bonds formed between water and the phosphate groups of the lipid molecules as well as among the water molecules themselves have been characterized in terms of two time correlation functions (TCFs), namely, the continuous hydrogen bond time correlation function,  $S(t)$ , and the intermittent hydrogen bond time correlation function,  $C(t)$ .<sup>4,18</sup> These TCFs are defined as

$$S(t) = \frac{\langle h(0)H(t) \rangle}{\langle h \rangle} \quad (1)$$

and

$$C(t) = \frac{\langle h(0)h(t) \rangle}{\langle h \rangle} \quad (2)$$

These definitions are based on two hydrogen bond population variables,  $h(t)$  and  $H(t)$ . The variable  $h(t)$  is unity when a particular pair of sites (phosphate–water or water–water) is hydrogen-bonded at time  $t$  according to the definition used and zero otherwise. The variable  $H(t)$ , however, is defined as unity, when the tagged pair of sites remain continuously hydrogen-bonded from time  $t = 0$  to time  $t$ , and zero otherwise. Thus,  $S(t)$  describes the probability that a hydrogen bond formed between two sites at time zero remains bonded at all times up to  $t$ . In other words,  $S(t)$  provides a strict definition of the lifetime of a tagged hydrogen bond. The correlation function,  $C(t)$ , however, describes the probability that a particular tagged hydrogen bond is intact at time  $t$ , given it was intact at time zero. Thus,  $C(t)$  is independent of the possible breaking of hydrogen bonds at intermediate times and allows reformation of broken bonds. In other words, it allows recrossing the barrier separating the bonded and nonbonded states as well as the long-time diffusive behavior. Therefore, the relaxation of  $C(t)$  provides information about the structural relaxation of a particular hydrogen bond.

We have calculated the time correlation function,  $C_{PW}(t)$ , for the hydrogen bonds formed between the lipid phosphate groups and the water molecules for both the mixed and pure bilayer systems. These are displayed in Figure 1a. The inset shows the corresponding function  $C_{WW}(t)$  for pure bulk water as well as for water present in the hydration layer of the lipid headgroups for both the simulation systems. The water molecules that reside within 4.5 Å from the phosphorus atoms of the lipid headgroups are considered to be within the first hydration layer. The distances are measured with respect to both the leaflets of the

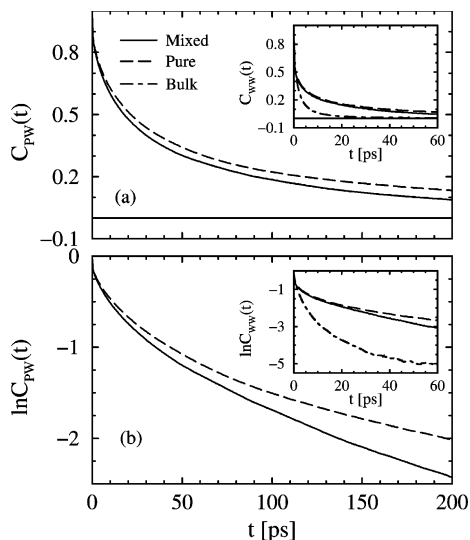


**Figure 1.** (a) Intermittent hydrogen bond time correlation function,  $C_{PW}(t)$ , between the lipid phosphate groups and the hydration layer water molecules for pure DMPC bilayer and mixed DMPC/ethanol bilayer systems. The inset shows the corresponding correlation function  $C_{WW}(t)$  for hydrogen bonds between water molecules present in the hydration layer of the lipid headgroups for both the simulation systems as well as for pure bulk water. The semilog plots of the corresponding functions are displayed in part b.

bilayer by tagging water molecules at different time origins. The results for bulk water have been obtained from a MD simulation of pure TIP3P water under identical conditions. Figure 1b shows the semilog plots of the corresponding correlation functions. It is apparent from the figure that the structural relaxation of the phosphate–water (PW) hydrogen bonds is much slower than that for the water–water (WW) hydrogen bonds in bulk water. Such slow relaxation behavior has been observed earlier for hydrogen bonds between the polar headgroups of surfactants and water molecules at a micellar interface<sup>25</sup> as well as at the interface of a surfactant monolayer.<sup>47</sup> This arises due to strong interaction between the lipid phosphate groups and the hydration layer water molecules. The calculated average phosphate–water hydrogen bond energies have been found to be  $-11.3$  kcal/mol for the mixed bilayer system and  $-11.7$  kcal/mol for the pure bilayer system. These energy values are much lower than the average hydrogen bond energy of  $-4.1$  kcal/mol for pure bulk water. Thus, the water molecules near the lipid headgroups are likely to remain significantly bound due to the formation of strong hydrogen bonds with the lipid phosphate groups. The presence of such strongly bound water molecules at the bilayer interface results in the slower relaxation of  $C_{PW}(t)$ . The slower relaxation of  $C_{WW}(t)$  for the hydration layer water molecules compared to pure bulk water, as shown

in the inset of Figure 1a, also arises due to the presence of such bound water molecules. However, more interestingly, we notice that the presence of ethanol modifies the relaxation behavior of  $C_{PW}(t)$ . The structural relaxation of phosphate–water hydrogen bonds is faster in the presence of ethanol. All of the decay curves show the presence of slow components at long times. Such slow long-time decay cannot be described by a single-exponential law. We have fitted the decay curves (Figure 1a) to multiexponentials, and the parameters for best fits along with the amplitude-weighted average time constants ( $\langle t_c \rangle$ ) are listed in Table 1. It may be noted that the  $\langle t_c \rangle$  values for phosphate–water hydrogen bonds are about 20–30 times longer than the water–water hydrogen bonds in pure bulk water. The corresponding values for the hydration layer water molecules are also significantly higher (3–5 times) than those for bulk water. Thus, the presence of strongly bound water molecules at the bilayer interface is clearly evident from these results. In our earlier study,<sup>36</sup> we noticed that both the translational and the rotational motions of the hydration layer water molecules are significantly restricted. Thus, we observe an excellent correlation between the relaxation behavior of the intermittent phosphate–water hydrogen bond TCF ( $C_{PW}(t)$ ) and the dynamics of the hydration layer water molecules. It is also observed that the  $\langle t_c \rangle$  values for phosphate–water hydrogen bonds is about 30% shorter in the presence of ethanol. This again correlates well with 15–20% higher mobility of hydration layer water molecules in the presence of ethanol.<sup>36</sup> It may be noted that ethanol, being a polar molecule like water, can form hydrogen bonds with the polar phosphate or carbonyl groups of the lipid. Hydrogen bonds between the ethanol and the phosphate groups are more important as the latter is more exposed to the aqueous layer. The relatively faster relaxation of phosphate–water hydrogen bonds and faster dynamics of hydration layer water molecules in the presence of ethanol can be explained in terms of the relative strengths of phosphate–water and phosphate–ethanol hydrogen bonds. The calculated average phosphate–water and phosphate–ethanol hydrogen bond energies in the mixed bilayer system have been found to be  $-11.3$  and  $-11.1$  kcal/mol, respectively. Therefore, the hydrogen bonds formed by water and ethanol with lipid phosphate groups are of almost equal strength. This suggests that water molecules forming hydrogen bonds with lipid phosphate groups can be easily exchanged with ethanol molecules without any energy cost. Thus, in the presence of ethanol, the water molecules are likely to form short-lived hydrogen bonds with lipid phosphate groups, which results in faster structural relaxation of phosphate–water hydrogen bonds. It may also be noted that the presence of ethanol at the interface can cause some structural distortion of phosphate–water hydrogen bonds. Such distortion along with a gain in entropy by water may also play a role in shortening

**TABLE 1: Multiexponential Fitting Parameters for the Phosphate–Water ( $C_{PW}(t)$ ) and Water–Water ( $C_{WW}(t)$ ) Intermittent Hydrogen Bond Time Correlation Functions for Both the Pure and the Mixed Bilayer Systems<sup>a</sup>**

system	PO <sub>4</sub> ···H <sub>2</sub> O			H <sub>2</sub> O···H <sub>2</sub> O		
	time constant (ps)	amplitude (%)	$\langle t_c \rangle$ (ps)	time constant (ps)	amplitude (%)	$\langle t_c \rangle$ (ps)
mixed	0.75	18.4	58.66	0.23	50.4	10.42
	17.27	39.9		5.19	27.1	
	123.81	41.7		39.53	22.5	
pure	1.05	20.0	81.37	0.26	50.7	14.10
	24.21	43.5		6.72	30.6	
	193.50	36.5		63.73	18.7	
bulk water				0.28	34.4	2.93
				2.34	54.6	
				14.11	11.0	

<sup>a</sup> Corresponding parameters for bulk water are also listed for comparison.  $\langle t_c \rangle$  is the average time constant.



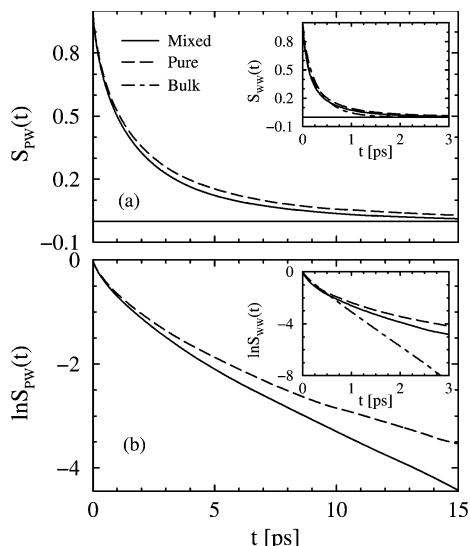


**Figure 2.** (a) Continuous hydrogen bond time correlation function,  $S_{PW}(t)$ , between the lipid phosphate groups and the hydration layer water molecules for pure DMPC bilayer and mixed DMPC/ethanol bilayer systems. The inset shows the corresponding correlation function  $S_{WW}(t)$  for hydrogen bonds between water molecules present in the hydration layer of the lipid headgroups for both the simulation systems as well as for pure bulk water. The semilog plots of the corresponding functions are displayed in part b.

the life of phosphate–water hydrogen bonds. However, this needs to be verified further.

In Figure 2a, we display the relaxation of the continuous hydrogen bond time correlation function,  $S_{PW}(t)$ , for the hydrogen bonds between the lipid phosphate groups and the hydration layer water molecules for both the simulation systems.

The inset shows the corresponding function  $S_{WW}(t)$  for pure bulk water as well as for water present in the hydration layer of the lipid headgroups. Figure 2b shows the semilog plots of the corresponding correlation functions. In all cases, a rapid initial decay in the correlation function arising primarily due to the fast librational and vibrational motions of the hydrogen-bonded sites have been observed. We notice that the relaxation of the function for phosphate–water hydrogen bonds ( $S_{PW}(t)$ ) is significantly slower than the corresponding function for water–water hydrogen bonds ( $S_{WW}(t)$ ). It is also noted that the function  $S_{PW}(t)$  relaxes slightly faster in the presence of ethanol. This is in accordance with the relaxation behavior of  $C_{PW}(t)$ , as observed earlier (Figure 1), and indicates shorter lifetimes of phosphate–water hydrogen bonds in the presence of ethanol. We have again fitted the decay curves (Figure 2a) to multiexponentials and listed the parameters for best fits as well as the amplitude-weighted average time constants ( $\langle t_s \rangle$ ) in Table 2. The calculated  $\langle t_s \rangle$  values for the phosphate–water hydrogen bonds

have been found to be approximately 7–10 times longer than that estimated for pure TIP3P water. It may be noted that the calculated  $\langle t_s \rangle$  value of 0.29 ps for water–water hydrogen bonds in pure TIP3P water is closer to the lower end of the experimental values of the characteristic hydrogen bond time constant, which vary between 0.3 and 0.7 ps.<sup>12</sup> As discussed before, the hydration layer water molecules form much stronger hydrogen bonds with phosphate groups and hence have longer lifetimes. Due to the presence of such strongly bound motionally restricted water molecules in the hydration layer, the average time constants of the hydrogen bonds between them are also found to be slightly longer than those of pure bulk water. From the above discussion, it is clear that the nonexponential nature is particularly significant for the dynamics observed in bilayer systems rather than in pure bulk water. As reported earlier for ionic micelles,<sup>25</sup> such relaxation behavior in bilayer systems may arise due to a constrained bonding arrangement at the interface. However, further verification is necessary to understand such complex behavior. It may be noted at this stage that we are currently investigating in detail the effect of ethanol at different concentrations on the dynamics of hydrogen bonds. The preliminary results indicate that the trends observed in the present work remain almost independent of ethanol concentration.

It is well-known that the dynamics of hydrogen bonds between two molecules is strongly coupled with the diffusion of the molecules.<sup>5,6,10,48</sup> Luzar and Chandler<sup>5</sup> have demonstrated that such coupling is the physical origin of the nonexponential relaxation of the hydrogen bond TCFs. Faster diffusion will result in faster hydrogen bond relaxation and vice versa. In this case, as the diffusion of the lipid molecules in the bilayer would be much slower than that of water, it is expected that the dynamics of phosphate–water hydrogen bonds will be correlated with the self-diffusion of hydration layer water molecules. Slower diffusion of water is expected to allow reformation of broken hydrogen bonds and hence will result in slower relaxation of phosphate–water hydrogen bonds. To eliminate the contribution arising from the diffusion of hydration layer water molecules, we calculate the time correlation function<sup>5,6,10,48,49</sup>

$$N(t) = \frac{\langle h(0)(1 - h(t))H'(t) \rangle}{\langle h \rangle} \quad (3)$$

for the phosphate–water hydrogen bonds.  $H'(t)$  is unity if the tagged pair of sites is closer than a cutoff distance,  $R_H$  (3.25 Å for phosphate–water and 3.5 Å for water–water hydrogen bonds) at time  $t$ , and zero otherwise. Thus a nonzero value for  $N(t)$  indicates that the tagged pair of sites are no longer hydrogen-bonded but remain in the vicinity of each other (i.e., within  $R_H$ ). A value of zero suggests that the two sites either

**TABLE 2: Multiexponential Fitting Parameters for the Phosphate–Water ( $S_{PW}(t)$ ) and Water–Water ( $S_{WW}(t)$ ) Continuous Hydrogen Bond Time Correlation Functions for Both the Pure and the Mixed Bilayer Systems<sup>a</sup>**

system	PO <sub>4</sub> ···H <sub>2</sub> O			H <sub>2</sub> O···H <sub>2</sub> O		
	time constant (ps)	amplitude (%)	$\langle t_s \rangle$ (ps)	time constant (ps)	amplitude (%)	$\langle t_s \rangle$ (ps)
mixed	0.18	17.1	2.20	0.06	34.5	0.32
	1.28	47.4		0.26	46.8	
	4.39	35.5		0.93	18.7	
pure	0.31	25.7	2.78	0.06	37.1	0.37
	2.10	56.9		0.32	46.7	
	8.65	17.4		1.25	16.2	
bulk water				0.06	22.3	0.29
				0.35	77.7	

<sup>a</sup> Corresponding parameters for bulk water are also listed for comparison.  $\langle t_s \rangle$  is the average time constant.

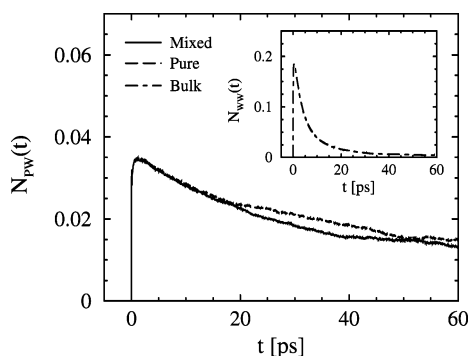


**Figure 3.** Time-dependent probability that a phosphate–water hydrogen bond is broken but the water molecule remains in the vicinity of the phosphate groups (i.e., within  $R_H$ ),  $N_{PW}(t)$ , for both pure DMPC bilayer and mixed DMPC/ethanol bilayer systems. The inset shows the corresponding function  $N_{WW}(t)$  for pure bulk water.

are in the bonded state or are separated by a distance larger than  $R_H$ . Thus,  $N(t)$  describes the time-dependent probability that a particular hydrogen bond between a pair of sites is broken at time  $t$ , but the two sites have not diffused away and remain as nearest neighbors. The relaxation of  $N(t)$  can occur due to reformation of the broken hydrogen bonds or due to diffusion (mainly rotational) of the two sites.<sup>5</sup>

In Figure 3, we display the relaxation of  $N_{PW}(t)$  for the hydrogen bonds formed between the lipid phosphate groups and the hydration layer water molecules for both the simulation systems. The corresponding function  $N_{WW}(t)$  for pure bulk water is displayed in the inset for comparison. The figure shows that the relaxation of  $N_{PW}(t)$  is much slower than that of  $N_{WW}(t)$ . This is a signature of the rigidity of the lipid hydration layer, which is in accordance with the slow relaxation of phosphate–water hydrogen bond TCFs (Figures 1 and 2). Interestingly, a small but noticeable change in the relaxation behavior of  $N_{PW}(t)$  is observed in the presence of ethanol. It is apparent that the lipid hydration layer becomes slightly less rigid in the presence of ethanol. This is an important observation and agrees well with the effects of ethanol on the dynamics of phosphate–water hydrogen bonds, as discussed before.

To further investigate the rigidity of the lipid hydration layer and its sensitivity to the presence of ethanol near the interface, we looked into the kinetics of breaking and reformation of phosphate–water hydrogen bonds in further detail. We adopt the simple model proposed by Luzar and Chandler<sup>5,6</sup> to describe the kinetics of breaking and formation of phosphate–water hydrogen bonds as



where B is the bound state, where a water molecule is hydrogen-bonded with phosphate groups, and QF is the quasi-free state, where the hydrogen bond is broken, but the water molecule remains within the first coordination shell of the phosphate group (i.e., within distance  $R_H$ ). As per the definitions, the probabilities  $C_{PW}(t)$  and  $N_{PW}(t)$  correspond to local populations of states B and QF, respectively, which can interconvert according to eq 4.<sup>5,6</sup> For a rigid hydration layer, where the diffusion is slow, the populations  $C_{PW}(t)$  and  $N_{PW}(t)$  can individually change by interconversion, but  $C_{PW}(t) + N_{PW}(t)$  should remain constant.<sup>5</sup> In Figure 4, we plot  $C_{PW}(t) + N_{PW}(t)$  for the phosphate–water hydrogen bonds separately for the two simulation systems. The inset shows the decay of the corresponding function for pure bulk water. It is clear that compared to bulk water the function relaxes slowly for the hydration layer water molecules of the bilayer systems. The relatively faster relaxation of the function

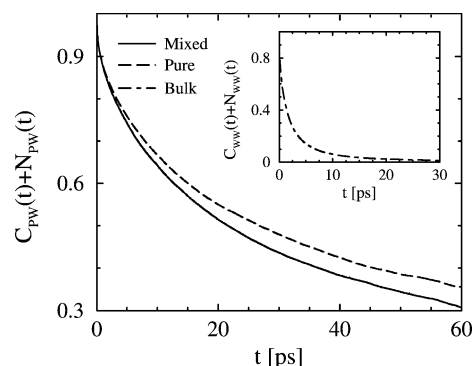


**Figure 4.** Relaxation of the function  $C_{PW}(t) + N_{PW}(t)$  for the phosphate–water hydrogen bonds for both the pure DMPC bilayer and the mixed DMPC/ethanol bilayer systems. The inset displays the corresponding function  $C_{WW}(t) + N_{WW}(t)$  for pure bulk water.

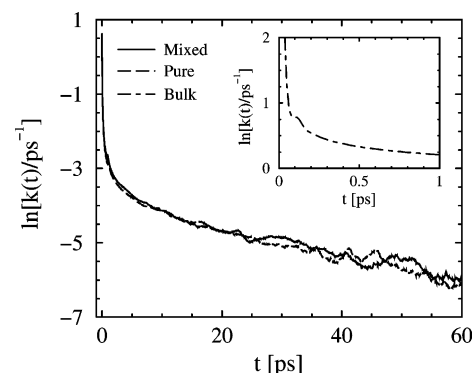


**Figure 5.** Phosphate–water hydrogen bond reactive flux,  $k(t)$  (semilog plot) for the breaking and reformation of hydrogen bonds between the lipid phosphate groups and the hydration layer water molecules, for both pure DMPC bilayer and mixed DMPC/ethanol bilayer systems. The inset shows the corresponding function for pure bulk water.

in the presence of ethanol indicates faster dynamics of the hydration layer water and lower interconversion between B and QF states. Thus the reformation of broken phosphate–water hydrogen bonds is less significant in the presence of ethanol. This makes the lipid hydration layer less rigid in the presence of ethanol.

Luzar and Chandler<sup>5,6</sup> proposed a simple model to describe the hydrogen bond kinetics in liquid water. Following their work, we attempt to connect the microscopic description of phosphate–water hydrogen bond dynamics and phenomenological reaction kinetics of their breaking and reformation, as shown in eq 4 for both the mixed and the pure bilayer systems. If  $k_1$  and  $k_2$  are the forward (breaking) and backward (reformation) rate constants, then a simple rate equation for the “reactive flux” can be written as

$$k(t) = -\frac{dC_{PW}(t)}{dt} = k_1 C_{PW}(t) - k_2 N_{PW}(t) \quad (5)$$

The relaxation of  $k(t)$  to equilibrium occurs by transitions from reactants to products, i.e., from state B to state QF (eq 4). We have calculated  $k(t)$  from the derivative of the simulated results of the intermittent hydrogen bond TCF,  $C_{PW}(t)$ , for the two simulation systems. This is displayed in Figure 5. At short times (transient period),  $k(t)$  relaxes fast for both of the systems, which arises due to fast librational and vibrational motions involving the hydrogen-bonded sites. The duration of this transient period for the phosphate–water hydrogen bonds is of same order as that for pure bulk water ( $\sim 0.2$  ps), as shown in the inset of Figure 5 and also reported in the literature.<sup>5</sup> The presence of

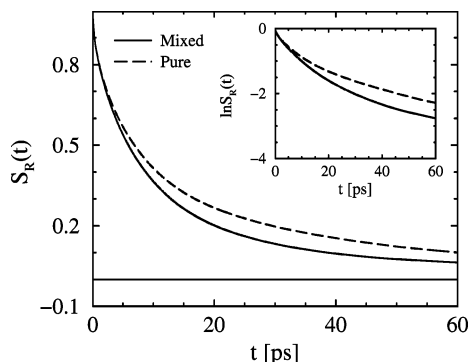


**Figure 6.** Residence time correlation function,  $S_R(t)$ , of water molecules present in the lipid hydration layer for both pure DMPC bilayer and mixed DMPC/ethanol bilayer systems. The inset shows the corresponding semilog plots.

**TABLE 3: Forward ( $k_1$ ) and Backward ( $k_2$ ) Rate Constants for Phosphate–Water Hydrogen Bond Breaking and the Average Hydrogen Bond Lifetime ( $1/k_1$  (ps)) as Obtained from a Least-Squares Fit of Eq 5 to the Simulation Results of Both the Pure and the Mixed Bilayer Systems**

system	$k_1$ (ps <sup>-1</sup> )	$k_2$ (ps <sup>-1</sup> )	$1/k_1$ (ps)
mixed	0.42	8.50	2.38
pure	0.33	6.71	3.03

ethanol did not show any clear influence on the relaxation behavior of  $k(t)$  beyond the transient period. We have used the least-squares fit approach<sup>10,49</sup> for  $t > 0.2$  ps to obtain the forward and backward rate constants ( $k_1$  and  $k_2$ ) that best satisfy eq 5 for the two systems. These are listed in Table 3. The inverse of the forward rate constant ( $1/k_1$ ), which corresponds to the average hydrogen bond lifetime, is also included in the table. It may be noted that the values of  $1/k_1$  are slightly larger than the  $\langle t_s \rangle$  values of phosphate–water hydrogen bonds, as obtained from  $S_{PW}(t)$ . This is expected, as  $S_{PW}(t)$  primarily provides information about the dynamics of hydrogen bond breaking due to fast librational and vibrational motions, while the quantity  $1/k_1$  additionally includes contributions from the slower mobility of hydration layer water molecules.<sup>49</sup> It may be noted that the macroscopic rate law (eq 5) cannot resolve short-time transient behavior and is applicable on a coarse-grained time scale. However, the correlation functions as shown in Figures 1 and 2 can provide valuable information on different time scales associated with the dynamics (Tables 1 and 2).

The effect of ethanol on the dynamics of hydrogen bonds at the bilayer interface and the rigidity of the hydration layer will be reflected in the average residence time of water as well as their number fluctuation in the hydration layer. We have analyzed the residence time of the hydration layer water molecules by measuring the time correlation function (TCF),  $S_R(t)$ , defined as

$$S_R(t) = \frac{\langle q(0)Q(t) \rangle}{\langle q \rangle} \quad (6)$$

The variable  $q(t)$  is unity when a particular water molecule is present within the hydration layer at time  $t$  and zero otherwise. The variable  $Q(t)$ , however, is defined as unity, when the tagged water molecule remains continuously within the hydration layer from time  $t = 0$  to time  $t$ , and zero otherwise. In Figure 6, we display the variation of  $S_R(t)$  versus time for both the simulation systems. The inset shows the semilog plots of the corresponding correlation functions. It is clear from the plots that the relaxation of  $S_R(t)$  is faster in the presence of ethanol. These decay curves are again fitted to multiexponentials to obtain an estimation of

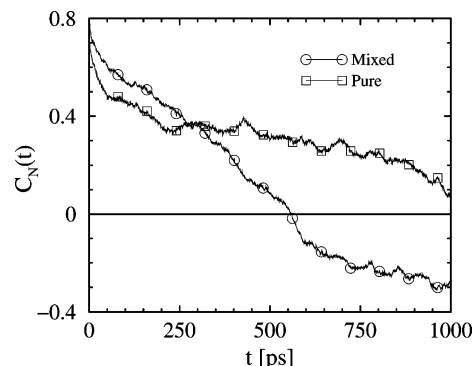


**Figure 7.** Fluctuation in the number of water molecules present in the lipid hydration layer for both pure DMPC bilayer and mixed DMPC/ethanol bilayer systems.

the average residence times. It is found that the average residence time of a water molecule in the hydration layer is 20.2 ps for the pure bilayer system and 15.3 ps for the mixed system. Thus the average residence time of a hydration layer water molecule decreases by  $\sim 25\%$  in the presence of ethanol. This again agrees with the relatively faster dynamics of phosphate–water hydrogen bonds and the lower rigidity of the hydration layer in the presence of ethanol. We have also calculated the number fluctuation correlation function,  $C_N(t)$ , defined as

$$C_N(t) = \frac{\langle \delta N(0)\delta N(t) \rangle}{\langle \delta N \rangle} \quad (7)$$

for the water molecules present in the lipid hydration layer. Here,  $\delta N(t) = N(t) - \langle N \rangle$ , where  $N(t)$  is the number of water molecules present in the hydration layer at time  $t$  and  $\langle N \rangle$  is the average number of water molecules present in the layer. Figure 7 shows the decay of the correlation function for the two simulation systems. It is evident from the figure that the function decays faster in the presence of ethanol. This is again in accordance with the lower rigidity of lipid hydration layer and relatively faster structural relaxation of phosphate–water hydrogen bonds due to the presence of ethanol molecules.

#### 4. Conclusions

In this article, we have explored in detail the effect of ethanol as an impurity on the hydrogen bond lifetime dynamics in the hydration layer of a DMPC lipid bilayer in its liquid crystalline lamellar ( $L_\alpha$ ) phase. The calculations are carried out by means of extensive atomistic MD simulations with 1:1 ethanol composition. In particular, we have studied the effects of the presence of ethanol near the bilayer interface on the dynamics of hydrogen bonds between the lipid phosphate groups and water. We have used the analysis of Luzar and Chandler<sup>5,6</sup> to obtain the rate constants that quantify the dynamic equilibrium between the bound and the free water molecules present in the lipid hydration layers. The results are compared with those corresponding to the pure DMPC bilayer system as well as that of water–water hydrogen bonds in bulk water. To the best of our knowledge, this is the first attempt to quantify the effects of ethanol on the phosphate–water hydrogen bond lifetime dynamics at the bilayer interface.

The calculations revealed that water molecules in the hydration layer of the bilayer form strong hydrogen bonds with lipid phosphate groups. This leads to slower relaxation of phosphate–water hydrogen bond TCFs compared to pure bulk water. The average time constants for the phosphate–water hydrogen bond



lifetimes were 7–10 times longer in both the pure and the mixed simulation systems than the corresponding value for bulk water. The long lifetime of the phosphate–water hydrogen bonds allows these bonded water molecules to be classified as “bound”. More interestingly, it is noticed that in the presence of ethanol the phosphate–water hydrogen bonds exhibit faster dynamics than that in the pure bilayer system. We have observed that both water and ethanol molecules are capable of forming hydrogen bonds of equal strength with lipid phosphate groups. Thus, the ethanol molecules present in the mixed system can easily replace the water molecules bound to the phosphate groups. This resulted in shorter lifetimes and hence faster structural relaxation of phosphate–water hydrogen bonds in the presence of ethanol. It has been noted that although the hydration layer of a lipid bilayer is highly rigid, the extent of rigidity decreases in the presence of ethanol as an impurity. This arises due to the faster relaxation of phosphate–water hydrogen bonds and higher mobility of hydration layer water molecules in the presence of ethanol. Adopting the simple model proposed by Luzar and Chandler,<sup>5,6</sup> we studied the kinetics of phosphate–water hydrogen bond breaking and reformation. We noticed that the reformation of broken phosphate–water hydrogen bonds is less significant in the presence of ethanol.

Thus, in this work we have attempted to establish a correlation between the introduction of ethanol molecules as an impurity in a phospholipid bilayer and its influence on the dynamics of phosphate–water hydrogen bonds and the rigidity of the lipid hydration layer. The relatively faster dynamics of hydrogen bonds at the bilayer interface and the lowering of the rigidity of the hydration layer might have important implications on the ethanol-induced intoxication of biomembranes. Currently, we are studying the effects of ethanol separately on the hydrogen bonds formed between water and the double-bonded and single-bonded lipid oxygen atoms. We are also investigating in atomistic detail the effects of ethanol at different concentrations on regular bilayer properties.

**Acknowledgment.** This work was supported in part by generous grants from the Department of Science and Technology, Council of Scientific and Industrial Research (CSIR), and the Department of Biotechnology, Government of India. J.C. thanks IIT, Kharagpur, and S.C. thanks CSIR for providing scholarships.

## References and Notes

- (1) Eisenberg, D.; Kauzmann, W. *The Structure and Properties of Water*; Oxford University Press: New York, 1969.
- (2) *Correlations and Connectivity, Geometric Aspects of Physics, Chemistry and Biology*; Stanley, H. E., Ostrowsky, N., Eds.; Kluwer Academic: Dordrecht, The Netherlands, 1990.
- (3) Teixeira, J. J. *Phys. IV C1* **1993**, 3, 162.
- (4) Stillinger, F. H. *Science* **1980**, 209, 451. Stillinger, F. H. *Adv. Chem. Phys.* **1975**, 31, 1.
- (5) Luzar, A.; Chandler, D. *Nature* **1996**, 397, 55. Luzar, A.; Chandler, D. *Phys. Rev. Lett.* **1996**, 76, 928.
- (6) Luzar, A. *J. Chem. Phys.* **2000**, 113, 10663. Luzar, A. *Chem. Phys.* **2000**, 258, 267.
- (7) Chen, S. H.; Teixeira, J. *Adv. Chem. Phys.* **1986**, 64, 1. *Hydrogen-Bonded Liquids*; Dore, J. C., Teixeira, J., Eds.; Kluwer Academic: Dordrecht, The Netherlands, 1991.
- (8) Blumberg, R. L.; Stanley, H. E. *J. Chem. Phys.* **1984**, 80, 5230. Sciortino, F.; Poole, P. H.; Stanley, H. E.; Havlin, S. *Phys. Rev. Lett.* **1990**, 64, 1686.
- (9) Ohmine, I.; Tanaka, H. *Chem. Rev.* **1993**, 93, 2545. Ohmine, I.; Saito, S. *Acc. Chem. Res.* **1999**, 32, 741.
- (10) Xu, H.; Stern, H. A.; Berne, B. J. *J. Phys. Chem. B* **2002**, 106, 2054.
- (11) Laenen, R.; Rauscher, C.; Laubereau, A. *Phys. Rev. Lett.* **1998**, 80, 2622.
- (12) Neinhuis, H. K.; Woutersen, S.; van Santen, R. A.; Bakker, H. J. *J. Chem. Phys.* **1999**, 111, 1494. Woutersen, S.; Emmerichs, U.; Bakker, H. J. *Science* **1997**, 278, 658. Kropman, M. F.; Bakker, H. J. *Science* **2001**, 291, 2118. Kropman, M. F.; Bakker, H. J. *J. Chem. Phys.* **2001**, 115, 8942.
- (13) Gale, G. M.; Gallot, G.; Hache, F.; Lascoux, N.; Bratos, S.; Leickman, J. C. *Phys. Rev. Lett.* **1999**, 82, 1068.
- (14) Danninger, W.; Zundel, G. *J. Chem. Phys.* **1981**, 74, 2769.
- (15) Walrafen, G. E. *J. Phys. Chem.* **1990**, 94, 2237.
- (16) Rousset, J. L.; Duval, E.; Boukenter, A. *J. Chem. Phys.* **1990**, 92, 2150.
- (17) Steinel, T.; Asbury, J. B.; Zheng, J.; Fayer, M. D. *J. Phys. Chem. A* **2004**, 108, 10957.
- (18) Rapaport, D. C. *Mol. Phys.* **1983**, 50, 1151.
- (19) Belch, A. C.; Rice, S. A. *J. Chem. Phys.* **1987**, 86, 5676.
- (20) Zichi, D. A.; Rossky, P. J. *J. Chem. Phys.* **1986**, 84, 2814.
- (21) Chandra, A. *Phys. Rev. Lett.* **2000**, 85, 768. Chandra, A. *J. Phys. Chem. B* **2003**, 107, 3899.
- (22) Luzar, A.; Chandler, D. *J. Chem. Phys.* **1993**, 98, 8160.
- (23) Starr, F. W.; Nielsen, J. K.; Stanley, H. E. *Phys. Rev. Lett.* **1999**, 82, 2294. Starr, F. W.; Nielsen, J. K.; Stanley, H. E. *Phys. Rev. E* **2000**, 62, 579.
- (24) Luzar, A. *Faraday Discuss.* **1996**, 103, 29.
- (25) Balasubramanian, S.; Pal, S.; Bagchi, B. *Phys. Rev. Lett.* **2002**, 89, 115505. Pal, S.; Balasubramanian, S.; Bagchi, B. *Phys. Rev. E* **2003**, 67, 061502.
- (26) Damodaran, K. V.; Merz, K. M. *Biophys. J.* **1994**, 66, 1076.
- (27) Tu, K.; Tobias, D. J.; Klein, M. L. *Biophys. J.* **1995**, 69, 2558. Tu, K.; Tobias, D. J.; Blasie, J. K.; Klein, M. L. *Biophys. J.* **1996**, 70, 595.
- (28) Gierula, M. P.; Takaoka, Y.; Miyagawa, H.; Kitamura, K.; Kusumi, A. *J. Phys. Chem. A* **1997**, 101, 3677. Gierula, M. P.; Takaoka, Y.; Miyagawa, H.; Kitamura, K.; Kusumi, A. *Biophys. J.* **1999**, 76, 1228.
- (29) Lopez, C. F.; Nielsen, S. O.; Klein, M. L.; Moore, P. B. *J. Phys. Chem. B* **2004**, 108, 6603.
- (30) Shinoda, W.; Shimizu, M.; Okazaki, S. *J. Phys. Chem. B* **1998**, 102, 6647.
- (31) Saiz, L.; Klein, M. L. *Biophys. J.* **2001**, 81, 204.
- (32) Moore, P. B.; Lopez, C. F.; Klein, M. L. *Biophys. J.* **2001**, 81, 2484.
- (33) Tu, K.; Tarek, M.; Klein, M. L.; Scharf, D. *Biophys. J.* **1998**, 75, 2123. Tu, K.; Klein, M. L.; Tobias, D. J. *Biophys. J.* **1998**, 75, 2147.
- (34) Koubi, L.; Tarek, M.; Klein, M. L.; Scharf, D. *Biophys. J.* **2000**, 78, 800. Koubi, L.; Saiz, L.; Tarek, M.; Scharf, D.; Klein, M. L. *J. Phys. Chem. B* **2003**, 107, 14500.
- (35) Chanda, J.; Bandyopadhyay, S. *Chem. Phys. Lett.* **2004**, 392, 249.
- (36) Chanda, J.; Bandyopadhyay, S. Unpublished work.
- (37) Petrache, H. I.; Nagle, S. T.; Nagle, J. F. *Chem. Phys. Lipids* **1998**, 95, 83.
- (38) Martyna, G. J.; Tuckerman, M. E.; Tobias, D. J.; Klein, M. L. *Mol. Phys.* **1996**, 87, 1117.
- (39) Tuckerman, M. E.; Yarne, D. A.; Samuelson, S. O.; Hughs, A. L.; Martyna, G. J. *Comput. Phys. Commun.* **2000**, 128, 333.
- (40) Darden, T.; York, D.; Pedersen, L. J. *J. Chem. Phys.* **1993**, 98, 10089.
- (41) Procacci, P.; Darden, T.; Marchi, M. *J. Phys. Chem.* **1996**, 100, 10464. Procacci, P.; Marchi, M.; Martyna, G. J. *J. Chem. Phys.* **1998**, 108, 8799.
- (42) Allen, M. P.; Tildesley, D. J. *Computer Simulation of Liquids*; Clarendon: Oxford, U. K., 1987.
- (43) Schlenkrich, M.; Brickmann, J.; MacKerell, A. D.; Karplus, M. Empirical Potential Energy Function for Phospholipids: Criteria for Parameter Optimization and Applications. In *Biological Membranes: A Molecular Perspective from Computation and Experiment*; Birkhauser: Boston, MA, 1996.
- (44) Jorgensen, W. L.; Chandrasekhar, J.; Madura, J. D.; Impey, R. W.; Klein, M. L. *J. Chem. Phys.* **1983**, 79, 926.
- (45) Mezei, M.; Beveridge, D. L. *J. Chem. Phys.* **1981**, 74, 622.
- (46) Stillinger, F. H.; Rahman, A. *J. Chem. Phys.* **1974**, 60, 1545.
- (47) Chanda, J.; Chakraborty, S.; Bandyopadhyay, S. *J. Phys. Chem. B* **2005**, 109, 471.
- (48) Xu, H.; Berne, B. J. *J. Phys. Chem. B* **2001**, 105, 11929.
- (49) Paul, S.; Chandra, A. *Chem. Phys. Lett.* **2004**, 386, 218.